AIAA 2004-5201

Recent Enhancements to USM3D Unstructured Flow Solver for Unsteady Flows

Mohagna J. Pandya
Swales Aerospace, Hampton, Virginia

Neal T. Frink and Khaled S. Abdol-Hamid
NASA Langley Research Center, Hampton, Virginia

James J. Chung
NAVAIR, Patuxent River, Maryland

22nd AIAA Applied Aerodynamics Conference & Exhibit
16-19 August 2004 / Providence, RI

Recent Enhancements to USM3D Unstructured Flow Solver for Unsteady Flows

Mohagna J. Pandya[*]
Swales Aerospace, Inc, Hampton, Virginia 23681

Neal T. Frink[†], Khaled S. Abdol-Hamid[†]
NASA Langley Research Center, Hampton, Virginia 23681

and

James J. Chung[‡]
NAVAIR, Patuxent River, Maryland 20670

The NASA USM3D unstructured flow solver is undergoing extensions to address dynamic flow problems in support of NASA and NAVAIR efforts to study the applicability of Computational Fluid Dynamics tools for the prediction of aircraft stability and control characteristics. The initial extensions reported herein include two second-order time stepping schemes, Detached-Eddy Simulation, and grid motion. This paper reports the initial code verification and validation assessment of the dynamic flow capabilities of USM3D. The cases considered are the classic inviscid shock-tube problem, low Reynolds number wake shedding from a NACA 0012 airfoil, high Reynolds number DES-based wake shedding from a 4-to-1 length-to-diameter cylinder, and forced pitch oscillation of a NACA 0012 airfoil with inviscid and turbulent flow.

Nomenclature

C_D	drag coefficient
C_L	lift coefficient
C_p	pressure coefficient
C_{pb}	pressure coefficient at leeward stagnation point of cylinder
c	reference chord or length
D	diameter of cylinder
ds	nominal distance between two adjacent grid nodes
f	frequency, Hertz
k-ε	kinetic energy-dissipation rate based two equation turbulence model
L	length
M_∞	freestream Mach number
p	pressure
Re	freestream Reynolds number
St	Strouhal number
t	time
U_∞	freestream velocity
u	streamwise velocity
x	axial distance
y^+	distance of first node from surface in boundary layer coordinate
α	angle-of-attack
α_{ampl}	amplitude of oscillations

---

* Research Engineer, Member, AIAA
† Research Engineer, Configuration Aerodynamics Branch, Mail Stop 499, Associate Fellow, AIAA
‡ Aerospace Engineer, Senior Member, AIAA

α_{mean}	mean angle of oscillations
Δt	non-dimensional time step
ρ	density
υ_t	eddy viscosity

Acronyms

ARSM	Algebraic Reynolds Stress Model
BC	boundary condition
DES	Detached Eddy Simulation
DOF	Degrees of Freedom
LES	Large Eddy Simulation
SA	Spalart-Allmaras turbulence model
URANS	Unsteady Reynolds-Averaged Navier-Stokes

I. Introduction

NASA Langley Research Center is engaged in a subproject called "Computational Methods for Stability and Control" (COMSAC) to coordinate activities among willing partners for exploring the applicability of computational fluid dynamics (CFD) tools in predicting the stability and control (S&C) characteristics of flight vehicles. The subproject is sponsored at Langley under the Efficient Aerodynamics and Shapes Integration (EASI) project, under the Vehicle Systems Program. A NASA symposium for COMSAC [1,2] held in Hampton, Virginia on September 23-25, 2003 brought together over 100 attendees from over 35 organizations to initiate dialog between the S&C and CFD communities, to begin assessment of the state-of-the-art in S&C prediction methods, and to explore how best to pool our resources and energies toward the COMSAC goals. While such a task is daunting, some promising activities and partnerships are beginning to emerge.

The Naval Air Systems Command (NAVAIR) and NASA Langley Research Center have joined together in a three-year cooperative effort to develop a computational modeling and simulation suite capable of handling air vehicle stability and control under the title of "Integrated Simulation of Air Vehicle Performance, Stability and Control for Test and Evaluation". NAVAIR was awarded funding and computer resources from the DoD High Performance Computing Modernization Office (HPCMO) under the Common High Performance Computing Software Support Initiative (CHSSI). This project is under Collaborative Simulation and Testing (CST) portfolio to provide scalable software for military applications to reduce risk in weapons system development and to provide information to senior decision makers throughout the life cycle of the system. The project goal is to integrate CFD analysis with flight simulation to demonstrate an improved test and evaluation process on fixed-wing air vehicle stability and control problems.

The joint NAVAIR/NASA commitment provides a substantial augmentation for improving the capabilities of an existing state-of-the-art computational system, known as TetrUSS [3], to enhance its ability to solve important problems for stability and control. While the NAVAIR focus is on military aircraft, NASA will maintain a parallel focus supporting civilian aircraft application. A primary thrust of this project will be the efficient computation of dynamic stability derivatives across an aircraft flight envelope for input into flight simulation programs. One fundamental requirement is for TetrUSS to be a validated, useable, robust system for computing unsteady, often massively separated flows on complex military and civilian aircraft configurations in dynamic motion.

Additional support for TetrUSS improvements is also coming from the U.S. ARMY Rotorcraft CFD project at NASA Langley. The goal is to explore the effectiveness of TetrUSS in analyzing existing and future rotorcraft configurations. TetrUSS was selected for this work in part because of its actuator disk boundary condition for modeling rotor effects. However, some additional enhancements common to the NAVAIR CHSSI project are needed for both unsteady and very low Mach number flows.

In support of these needs, work is presently underway to enhance, customize, and validate TetrUSS capabilities toward ready computation of dynamic derivatives across the flight envelope and the prediction of rotorcraft aerodynamics. The primary support will include the implementation and validation of second-order time accuracy, Detached Eddy Simulation (DES), a forced oscillation and 6-DOF free-to-roll (FTR) analysis capability, low-Mach number preconditioning, a suite of advanced two-equation turbulence models, Chimera overset moving grids, and assessments of code scalability across multiple computer platforms. Work is well underway for each of the above capabilities. A series of reports are planned over the next three to four years for documenting their validations and applications to COMSAC and rotorcraft related problems.

This paper will document the initial enhancements to the TetrUSS flow solver, USM3D, for second-order time accuracy, Detached Eddy Simulation, and dynamic grid motion through progressive verification and validation of those features. The initial assessment of the second-order time stepping will be conducted on the classic inviscid shocktube wave propagation problem followed by an examination of low Reynolds number wake shedding from a NACA 0012 airfoil at high angle of attack. The more complex hybrid DES methodology will be tested on a 4-to-1 length-to-diameter cylinder 3D wake shedding case. Finally, the dynamic-grid capability will be verified on a quasi-3D NACA 0012 airfoil in pitch oscillation using inviscid and turbulent flow.

II.   Description of Methodology

The NASA Tetrahedral Unstructured Software System (TetrUSS) [3] is a complete flow analysis system that has been widely used in industry and government since 1991. Its strength is derived from harnessing various component technologies into a user-friendly system to provide rapid, higher-order analysis and design capability to the applied aerodynamicist. TetrUSS consists of loosely integrated, user-friendly software that comprises of a geometry setup tool GridTool [4], a tetrahedral grid generator VGRIDns [5,6], a flow solver USM3D [7,8], and post-processing visualization and data extraction utilities. The system maintains sufficient flexibility that other researchers can utilize various components, such as grid generation, to support their codes as well. The subject extensions addressed in this paper pertain to the USM3D flow solver and will be described below.

A. USM3D Flow Solver

USM3D [7,8] is a tetrahedral cell-centered, finite volume Euler and Navier-Stokes (N-S) flow solver. Inviscid flux quantities are computed across each cell face using Roe's [9] flux-difference splitting (FDS). Spatial discretization is accomplished by a novel reconstruction process [10], which is based on an analytical formulation for computing solution gradients within tetrahedral cells. The solution is advanced in time by an implicit backward-Euler time-stepping scheme [11] with local time-stepping convergence acceleration for steady-state problems.

USM3D has several closure models for capturing flow turbulence effects. First is the Spalart-Allmaras (SA) one-equation model [12], which can be coupled with a wall function boundary condition to reduce the number of cells in the sublayer region of the boundary layer. However, the wall function is typically used only when extensive curvature-based separation is not expected in a flow simulation. The second model is the two-equation k-ε turbulence model [13,14]. The third model is the Menter SST two-equation model [15]. These turbulence models have undergone rigorous testing on propulsion afterbody flows in reference [16]. Two nonlinear Algebraic Reynolds Stress Models (ARSM) by Girimaji [17], and Shih/Zhu/Lumley [18], have recently been installed in USM3D and are undergoing verification testing.

USM3D supports an array of useful boundary conditions (BC's). It contains the standard BC's of flow tangency or no-slip on solid surfaces, characteristic inflow/outflow for subsonic boundaries, and freestream inflow and extrapolation outflow for supersonic flow. But it also contains some additional special BC's for jet exhaust and intake, a propeller/rotor actuator disk model, and passive porosity [19].

USM3D runs on massively parallel computers and clusters of personal computers (PC's). A grid partitioning file is quickly generated during a preprocessing step. A global restart file is generated and saved during and after each run. Thus, the user may readily change the number of processors from one restart run to the next if desired. The solver requires 175 eight-bit words of memory per tetrahedron. Solution run time is approximately 230 microsecond/cell/cycle/processor on an SGI Origin 2000 parallel computer.

B. Unsteady Extensions to USM3D

1. Second-Order Accuracy in Time

Second-order time-stepping is an established technique for improving the time-accuracy of conventional numerical schemes for unsteady flow computations. This strategy requires storing solution information at prior time levels and performing a subiteration of the solution between time steps to synchronize all cell properties at the next time level.

Two second-order time-stepping schemes have been implemented into USM3D. The first is a Crank-Nicholson scheme [20] which has the advantage of only *one prior time level* of the solution residual needing storage with a penalty of 6 words per cell. Some robustness problems were encountered with this approach, thus a three-point backward differencing scheme [21] was added. The three-point backward difference approach appears to be more robust but requires the additional storage of *two time-levels* of preceding flow variables with a penalty of 12 words per cell. However, the availability of parallel computer clusters with a gigabyte of memory on each processor is rapidly rendering CFD memory limitations to be a nonissue.

2. Detached Eddy Simulation

The difficult S&C problems occur at the edge-of-envelope flight conditions characterized by highly nonlinear, massively separated flows. Flow solvers based on the Unsteady Reynolds-Averaged Navier-Stokes (URANS) equations with standard turbulence closure models are not adequate in such extreme cases because of their intentional design to account for the entire spectrum of turbulent motions. Massively separated flows are characterized by unsteady geometry-dependent and three-dimensional turbulent eddies which the URANS turbulence models inherently diffuse. The full direct numerical simulation of both geometry-based and eddy-based separations on complex configurations is prohibitively expensive with current computer technology.

A clever interim solution to this shortcoming was proposed by Spalart, et al. [22] called Detached Eddy Simulation (DES) and is implemented via a small modification to the SA turbulence model [12]. The DES approach creates a hybrid model that attempts to combine the most favorable elements of URANS models and Large Eddy Simulation (LES). The standard SA model contains a wall-distance based destruction term to reduce the turbulent viscosity in the laminar sub layer and the log layer. By a simple modification of the wall-distance parameter away from the surface to reflect the local cell size in the field, the near-surface properties of the URANS model can be preserved while transitioning to a LES model away from the surface. The DES approach has been implemented into USM3D in accordance to the guidelines and experiences of Refs. 22 and 23.

3. Dynamic Grids

Grid motion capability has been added to USM3D to facilitate aerodynamic analysis of configurations undergoing unsteady motion. The immediate need is to compute the dynamic stability derivatives for pitch and roll oscillations for the COMSAC configurations.

The extensions primarily involved the simple addition of grid speed to the inviscid flux terms and boundary conditions within the flow solver. This modification is adequate for grids undergoing rigid-body motion. The Geometric Conservation Law (GCL) has also been implemented, although not used for present computations, to correct for flux errors encountered on deforming grids. All of these extensions were straightforward, but the dissertations of Singh [24], and Uzun [25] were used for guidance during the implementation. The input format to USM3D has been extended to allow user prescription of rigid-body sinusoidal motion in pitch, roll, or yaw.

III.   Results and Discussion

The following sections present the initial assessments of the USM3D modifications for unsteady flows. The initial assessment of the second-order time stepping will be conducted on the classic inviscid shocktube wave propagation problem followed by an examination of low Reynolds number wake shedding from a NACA 0012 airfoil at high angle of attack. The more complex high Reynolds number DES methodology will be tested on a 4-to-1 cylinder undergoing 3D wake shedding. Finally, the dynamic-grid capability will be verified on a quasi-3D NACA 0012 airfoil in pitch oscillation using inviscid and turbulent flow.

A. Wave Propagation

The initial verification and validation of the second-order time stepping scheme has been conducted on the classic shocktube problem for which an analytical solution also exists. Figure 1 shows the surface grid on a shocktube that is constructed as a 3D cylinder of length $L=1$. The grid, suitable for inviscid flow analysis, consists of 21,903 cells, 4,915 nodes and 4,558 boundary faces. The shocktube is closed at both the ends, and on all the surfaces of the shocktube tangent-flow solid wall boundary condition is imposed. Initial flow conditions are prescribed as shown below. These quantities have been non-dimensionalized with freestream values for density ρ_∞ and speed of sound a_∞ and a reference length L_{ref}.

$$\rho = 1.0, \quad p = 1.0, u = 0 \qquad 0.0 <= x < \ 0.5$$
$$\rho = 0.125, \ p = 0.1, u = 0 \qquad 0.5 <= x <= 1.0$$

The second-order Crank-Nicholson and 3-point backward-difference schemes are compared with a first-order solution in Fig. 2. The three solutions were each advanced for 100 time steps with a time (non-dimensionalized with ρ_∞, a_∞, and L_{ref}) increment of 0.002. Figure 2 shows a comparison of the transient density, pressure, streamwise velocity and Mach number profiles along the length of the shocktube corresponding to the computed and analytical solutions at time 0.2. It is evident that the computed solutions generally capture all the flow features of this problem, such as an expansion fan, contact discontinuity and a shock, with good accuracy relative to the exact solution. Furthermore, the improved accuracy of the second-order schemes is apparent in comparison to the first-order solution.

American Institute of Aeronautics and Astronautics Paper 2004-5201

B. Low Reynolds Number Airfoil Wake Shedding

The second problem considers the laminar-flow wake shedding from a NACA 0012 airfoil for a freestream Mach number of 0.3 at an angle-of-attack of 20-degree and chord Reynolds number of 3,000. For this problem, a quasi 3-D simulation of a 2-D problem has been performed and a narrow rectangular wing made up of NACA 0012 airfoil cross-sections between two endwalls has been considered. The wing has chord of unit length and span equivalent to 4% of the chord. The laminar grid for this case consists of 143,204 tetrahedral cells, 37,247 nodes and 53,156 boundary faces. Average grid spacing of the first layer of nodes from the wing surface is 0.1% of the chord. The side-plane grid distribution around the wing is shown in Fig. 3. Note that additional grid clustering has been inserted in the wake region.

Flow computations for this case have been performed using the 3-point backward-difference method. Computed solutions have been obtained for this case using three different non-dimensional time steps of 0.10, 0.05 and 0.025. At every unsteady time step, five subiterations have been performed to reduce the residual error by approximately one-and-a-half orders of magnitude. Figure 4 presents a history of the lift and drag coefficients for this case. A regular modulation of the force coefficients is established after 60 units of non-dimensional time that indicates a periodic shedding of vortices. A time step of 0.05 corresponds to an average of 127 points in each vortex shedding cycle. The computed Strouhal numbers ($St = fcSin\alpha / U_\infty$) corresponding to the time steps of 0.10, 0.05 and 0.025 are 0.173, 0.180 and 0.180, respectively. For comparison, Rumsey, et al. [26] computed a Strouhal number of 0.163 with a time step of 0.01 for the same case on a structured grid. The computed numbers are in the range of the general Strouhal number of about 0.150 reported by Tyler [27] for airfoils between 20- and 90-degree angle of attack. Figure 5 delineates the instantaneous flow field around the airfoil corresponding to the minimum- and maximum lift coefficient instances (t = 96.75 and 99.30, respectively) via pressure contours shown in close up view.

C. 3D Cylinder Wake Flow

The DES-based hybrid URANS/LES methodology is assessed on a 4-to-1 circular cylinder. The tetrahedral grid was obtained from Dr. James Forsythe of Cobalt Solutions, Inc. and has been used by Hansen and Forsythe [23] as the base grid; in their study, the grid was postprocessed into a prismatic grid within the boundary layer region. The full tetrahedral grid was used for the present work and has 2,003,873 cells, 350,304 nodes and 51,796 boundary faces. The grid has 23 nodes (69 tetrahedra) across the boundary layer in the body-normal direction and average grid spacing of the first layer of nodes from the cylinder is equivalent to $y^+ = 0.1$ The grid distribution in one side-plane of the cylinder is shown in the Figure 6.

Following the work of Travin, Shur, Strelets and Spalart [28], a DES flow computation was performed on the cylinder for a freestream Mach number of 0.1 and Reynolds number of 140,000 to simulate the turbulent separation (TS) flow case. The cylinder is mounted on two end walls where a reflection plane boundary condition has been applied. For this case, the 3-point backward-difference scheme has been used with a non-dimensional time step of 0.3 that corresponds to about 250 points in each shedding cycle. Each time step is resolved by five subiterations to produce an intermediate residual reduction of about two orders of magnitude. The computed history of the lift- and drag coefficients has been presented in Fig. 7.

The flow solution has been time-averaged between time intervals of 1500 to 8000 providing averaging over last 85 cycles. The computed distribution of the time-averaged surface pressure coefficients on a mid-span section of the cylinder has been compared with two experiments of Roshko [30] and van Nunen [31] in Fig. 8. The time-averaged drag coefficient, rear stagnation point pressure coefficient and Strouhal number from the present computation have been compared with those from measurements and other computations in Table 1. Based on the results listed in Table 1 and the comparisons of Fig. 8, it has been concluded that the current DES results compare well with experimental data and with other CFD simulations. A view of an instantaneous flow field is offered in Fig. 9 that shows an iso-surface of vorticity magnitude and eddy viscosity field in one cross-section corresponding to the solution at time = 8,000.1 units. The figure clearly shows that fine scales of motions have been captured by the computed solution.

In future work, we plan to explore a new approach to improve the accuracy and robustness of a simulation of an unsteady flow field based on the work presented in Ref. 29. One of the known deficiencies associated with current hybrid schemes such as DES is that because of the direct dependence of the model on local cell size, there is no clear identification of the different flow regions in the field. Several researchers observed that in most cases with hybrid methods, the use of a fine grid might result in incorrect simulations. Reference 29 offers an approach to clearly define regions as appropriate for URANS or DES in order to achieve a complete simulation that is independent of grid resolution.

Table 1. Cylinder in Cross-Flow, Mach=0.1, Re$_D$=140,000 TS Time-Averaged Results

Method	C$_D$	-C$_{pb}$	St
USM3D-DES	**0.72**	**0.84**	**0.27**
3D-DES Travin et al. [28]	0.57	0.65	0.3
Hansen and Forsythe [23]	0.59	0.72	0.29
PAB3D kε [29]	0.62	0.68	0.27
Experiment [30,31]	0.62-0.74	0.5-0.9	0.27

D. NACA 0012 Pitching Airfoil

The NACA 0012 airfoil has been experimentally tested in ramp and oscillatory pitch motions about the quarter-chord point at Aircraft Research Association Ltd, England. The results from the tests conducted at several freestream and pitch conditions have been reported in an AGARD report by Landon [32]. The unsteady flow prediction capability of USM3D has been assessed using the AGARD CT case 1 that corresponds to the test at a freestream Mach number of 0.6 and chord Reynolds number of 4.8×10^6. The angle-of-attack variation is prescribed as follows:

$$\alpha(t) = \alpha_{mean} + \alpha_{ampl} \, Sin(2\pi f t) \text{ where } \alpha_{mean} = 2.89°, \, \alpha_{ampl} = 2.41° \text{ and } f = 50.34 \text{ Hz.}$$

For this problem, a quasi 3-D simulation of a 2-D problem has been performed and a narrow rectangular wing made up of NACA 0012 airfoil cross-sections between two endwalls has been considered. The wing has a chord of unit length and span equivalent to 4% of the chord. Initially, two tetrahedral unstructured grids suitable for inviscid and viscous turbulent flow simulation have been generated. The inviscid grid consists of 134,909 tetrahedral cells, 35,370 nodes and 50,032 boundary faces whereas the viscous grid consists of 714,406 tetrahedral cells, 142,764 nodes and 93,410 boundary faces. The viscous grid has 25 points (75 tetrahedra) in the boundary layer and average spacing of the first layer of nodes from the wing surface is 5.3×10^{-6} yielding $y^+ = 1$. Both inviscid and viscous grids, have identical number of triangles on the wing surface which have been designated as *medium* inviscid and *medium* viscous grid, respectively.

A time step sensitivity study has been performed for both, inviscid and viscous simulations by selecting time steps equivalent to 200, 400 and 800 sample points per pitch cycle. The sensitivity of the flow solution has been assessed by monitoring the variation of force coefficients with respect to the angle-of-attack. The inviscid simulation displayed almost no sensitivity to the time step size in the selected range. However, for the viscous simulation 800 sample points per pitch cycle had to be used as larger values of time step introduced noise in the computed force coefficients.

Grid sensitivity for the viscous simulation has also been assessed using a *fine* viscous grid that has twice the number of tetrahedral cells and twice the number of triangular faces on the wing surface as for the *medium* viscous grid. The flow analysis on the *fine* viscous grid has been performed with the time step equivalent to 800 sample points per pitch cycle.

All the numerical solutions have been computed for three pitch cycles. The computed solutions have attained periodicity after two cycles. Figure 10 displays the comparisons of computed and measured histories of lift coefficient and pitching moment coefficient. It is evident from Fig. 10 that the solutions based on the *medium* and the *fine* viscous grids are almost identical. The instantaneous pressure coefficient contours based on the viscous computations in the near field of the airfoil have been presented in Fig. 11 corresponding to the minimum ($\alpha = 0.48°$) and maximum pitch angle ($\alpha = 5.3°$).

IV. Summary

NASA and NAVAIR are engaged in a three-year partnership to develop an improved computational test and evaluation process for addressing fixed-wing air vehicle stability and control problems. One requirement of the system is that it must be capable of analyzing dynamic stability and control problems occurring at edge-of-envelope

flight conditions often characterized by highly nonlinear, massively separated flows. In support of this project, work is presently underway to prepare the NASA TetrUSS suite of software for performing unsteady aerodynamic analysis of vehicles across the flight envelope. The primary extensions will include the implementation and validation of second-order time accuracy, Detached Eddy Simulation, a forced oscillation and 6-DOF free-to-roll analysis capability, low-Mach number preconditioning, a suite of advanced two-equation turbulence models, Chimera overset moving grids, and assessments of code scalability across multiple computer platforms.

This paper documents the initial enhancements to the TetrUSS flow solver, USM3D. Two second-order time stepping schemes have been added and shown to have good accuracy in wave propagation using the classic inviscid shocktube problem. The accuracy of the second-order schemes have been further verified for low-Reynolds number wake shedding on a NACA 0012 airfoil, and for high-Reynolds number wake shedding from a cylinder. For each of these cases, solution accuracies comparable to those of other structured and unstructured codes have been achieved. Finally, the dynamic-grid capability has been verified on a quasi-3D NACA 0012 airfoil in pitch oscillation for inviscid and turbulent flows.

Additional validation studies are currently underway for Detached Eddy Simulation and full aircraft dynamic stability derivatives on unit problems as well as the COMSAC configurations. As experience is gained, we plan to explore an emerging approach for reducing the grid dependence of the accuracy of separated flow simulations.

Acknowledgments

References

1. Fremaux, C.M. and Hall, R.M., Compilers, "COMSAC: Computational Methods for Stability and Control," NASA/CP-2004-213028/PT1, April 2004, pp. 361.
2. Fremaux, C.M. and Hall, R.M., Compilers, "COMSAC: Computational Methods for Stability and Control," NASA/CP-2004-213028/PT2, April 2004, pp. 413.
3. Frink, N.T., Pirzadeh, S.Z., Parikh, P.C., and Pandya, M.J., "The NASA Tetrahedral Unstructured Software System (TetrUSS)," *The Aeronautical Journal,* Vol.104, No. 1040, October 2000, pp. 491-499.
4. Samareh, J., "GridTool: A surface modeling and grid generation tool," Proceedings of the Workshop on Surface Modeling, Grid Generation, and Related Issues in CFD Solutions," NASA CP-3291, 9-11 May, 1995.
5. Pirzadeh, S., "Structured Background Grids for Generation of Unstructured Grids by Advancing Front Method," *AIAA Journal*, Vol. 31, No. 2, February 1993, pp. 257-265.
6. Pirzadeh, S., "Unstructured Viscous Grid Generation by Advancing-Layers Method," *AIAA Journal*, Vol. 32, No. 8, August 1994, pp. 1735-1737.
7. Frink, N. T., "Upwind Scheme for Solving the Euler Equations on Unstructured Tetrahedral Meshes," *AIAA Journal*, Vol., No. 1, January 1992, pp. 70-77.
8. Frink, N. T., "Tetrahedral Unstructured Navier-Stokes Method for Turbulent Flows," *AIAA Journal*, Vol. 36, No. 11, November 1998, pp. 1975-1982.
9. Roe, P., "Characteristic Based Schemes for the Euler Equations," *Annual Review of Fluid Mechanics*, Vol. 18, 1986, pp. 337-365.
10. Frink, N. T., "Recent Progress Toward a Three-Dimensional Unstructured Navier-Stokes Flow Solver," AIAA 94-0061, January 1994.
11. Anderson, W.; and Bonhaus D., "An Implicit Upwind Algorithm for Computing Turbulent Flows on Unstructured grids," *Computers Fluids*, Vol. 23, No. 1, 1994, pp. 1-21.
12. Spalart P., and Allmaras S. A., "One-Equation Turbulence Model for Aerodynamic Flows," AIAA Paper 92-0439, January 1992.

13. Jones,W. P., and Launder, B. E., "The Prediction of Laminarization With a Two-Equation Model of Turbulence," *Int. J. Heat & Mass Transf.*, Vol. 15, No. 2, February 1972, pp. 301-314.
14. Sarkar, S., Erlebacher, G., Hussaini, M. Y., and Kreiss, H. O., "The Analysis and Modeling of Dilatational Terms in Compressible Turbulence," *J. Fluid Mech.*, Vol. 227, June 1991, pp. 473-495.
15. Menter, F.R., "Improved Two-Equation k-omega Turbulence Models for Aerodynamic Flows", NASA TM-103975, October 1992.
16. Abdol-Hamid, K. S., Frink, N. T., Deere, K. A., and Pandya, M.J., "Propulsion Simulations Using Advanced Turbulence Models with the Unstructured-Grid CFD Tool, TetrUSS," AIAA Paper 2004-0714, January 2004.
17. Girimaji, S.S., "Fully-Explicit and Self-Consistent Algebraic Reynolds Stress Model," ICAS Report 95-82, 1995.
18. Shih, T-H, Zhu, J., and Lumley, J.L., "A New Reynolds Stress Algebraic Model," NASA TM-166614, ICOMP 94-8, 1994.
19. Frink, N.T., Bonhaus, D.L., Vatsa, V.N., Bauer, S.X.S, Tinetti, A.F., "A Boundary Condition for Simulation of Flow Over Porous Surfaces", *Journal of Aircraft*, Vol. 40, No. 4, July-August 2003, pp. 692-698.
20. Luo, H., Baum, J.D., Lohner, R., "An Accurate, Fast, Matrix-Free Implicit Method for Computing Unsteady Flows on Unstructured Grids," AIAA Paper No. 99-0937, January 1999.
21. Rumsey, C.L., Sanetrik, M.D., Biedron, R.T., Melson, N.D., Parlette, E.B., "Efficiency and Accuracy of Time-Accurate Turbulent Navier-Stokes Computations", *Computer & Fluids*, Vol. 25, No. 2, pp. 217-236, 1996.
22. Spalart, P.R., Jou, W-H, Strelets, M., and Allmaras, S.R., "Comments on the Feasibility of LES for Wings, and on a Hybrid RANS/LES Approach, Advances in DNS/LES," 1st AFOSR International Conference on DNS/LES, Greyden Press, Columbus, OH, 1997.
23. Hansen, R. P., and Forsythe, J. R., "Large and Detached Eddy Simulations of a Circular Cylinder Using Unstructured Grids," AIAA Paper 2003-0775, January 2003.
24. Singh, K.P., "Dynamic Unstructured Method for Prescribed and Aerodynamically Determined Relative Moving Boundary Problems", Ph.D. Dissertation for Old Dominion University, August 1995.
25. Uzun, A., "Parallel Computations of Unsteady Euler Equations on Dynamically Deforming Unstructured Grids", Master of Science Thesis for Purdue University, August 1999.
26. Rumsey, C.L., Thomas, J.L., Warren, G.P., and Liu, G.C., "Upwind Navier-Stokes Solutions for Separated Periodic Flows," *AIAA Journal*, Vol. 25, No. 4, April 1987, pp. 535-541.
27. Tyler, E., "Vortex Formation Behind Obstacles of Various Sections," *Philosophical Magazine S.7*, Vol. 11, No. 72, 1931, pp. 849-890.
28. Travin, A., Shur, M., Strelets, M., and Spalart, P., "Detached-Eddy Simulations Past a Circular Cylinder," *Flow Turbulence and Combustion*, Vol. 63, 1999, pp. 293-313.
29. Elmiligui, A., Abdol-Hamid, K. S., Massey, S. J., and Pao, S. P., "Numerical Study of Flow Past a Circular Cylinder Using RANS, Hybrid URANS/LES and PANS Formulations," AIAA Paper 2004-4959, August 2004.
30. Roshko, A., "Experiments on the Flow a Circular Cylinder at Very High Reynolds Number," *Journal of Fluid Mechanics*, Vol 10, No. 3, 1961, pp. 345-356.
31. van Nunen, J. W. G., "Pressure and Forces on a Circular Cylinder in a Cross Flow at High Reynolds Numbers," in Naudasher, E. (ed.), *Flow Induced Structural Vibrations*, Springer-Verlag, Berlin, 1974, pp. 748-754.
32. Landon, R., "Data Set 3 NACA 0012 Oscillatory and Transient Pitching," AGARD Report 702, AGARD, January 1982.
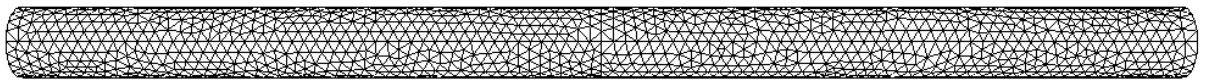
100 points along length of tube
L = 1, ds = 0.01

Figure 1. Outer surface triangulation on shocktube cylinder grid containing 21,903 tetrahedral cells.

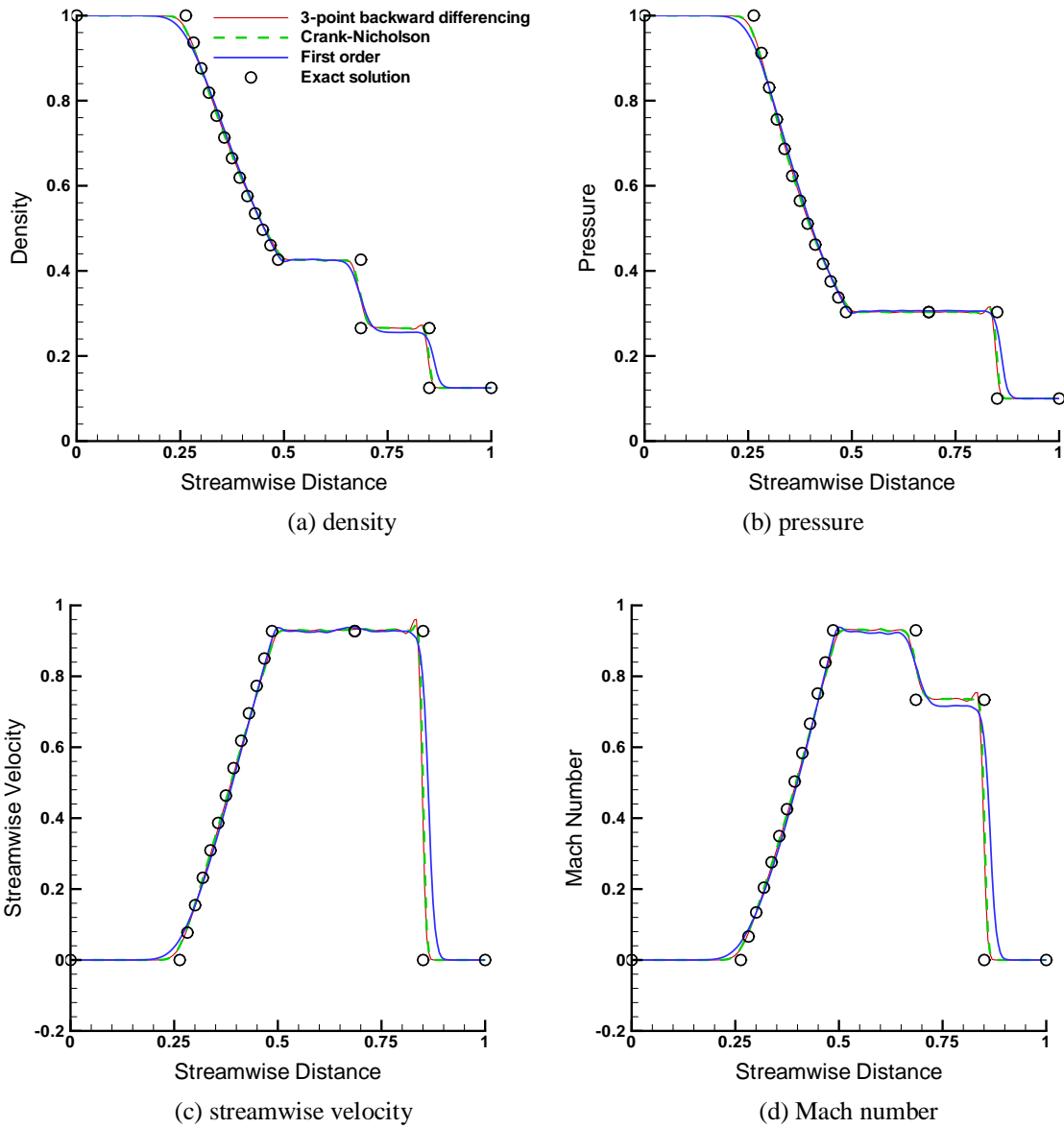(a) density

(b) pressure

(c) streamwise velocity

(d) Mach number

Figure 2. Comparison of USM3D and exact solutions at time 0.2 for a shock tube wave propagation after 100 time steps with non-dimensional Δt=0.002.
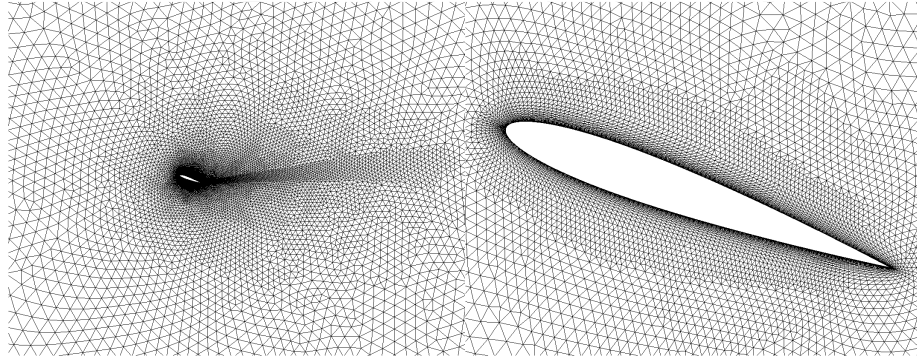
Figure 3. Side plane triangulation for NACA 0012 rectangular wing grid containing 143,204 tetrahedral cells.
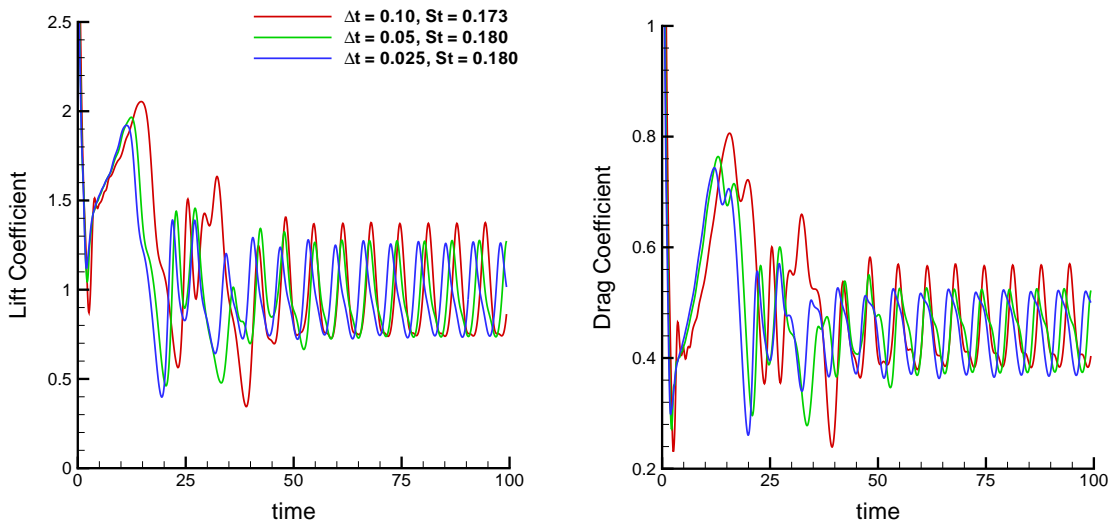
Figure 4. Computed history of the lift and drag coefficients for the laminar unsteady flow over NACA0012 rectangular wing at $M_\infty = 0.3$, $\alpha = 20°$, $Re_c = 3000$.

(a) close up view at minimum C_L instance

(b) close up view at maximum C_L instance
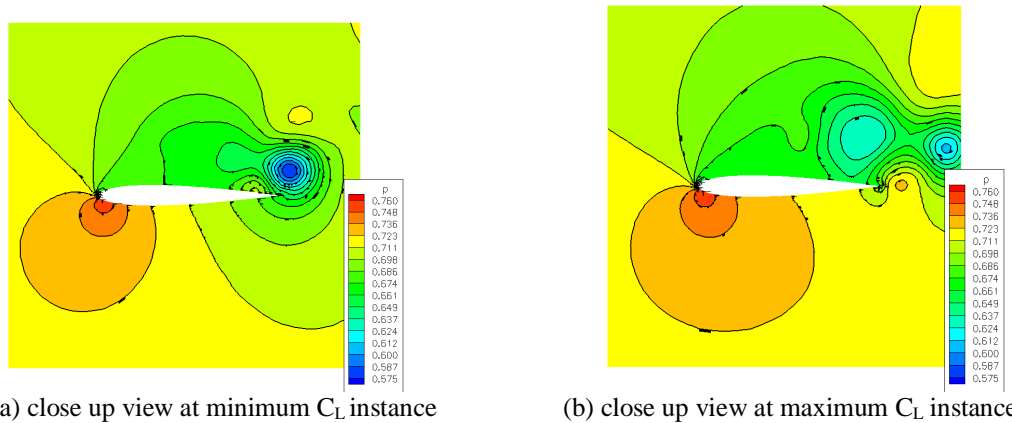
Figure 5. Instantaneous flow field around NACA 0012 rectangular wing at $M_\infty = 0.3$, $\alpha = 20°$, $Re_c = 3000$. (a) corresponds to minimum $C_L = 0.7357$, time = 96.75 units; (b) corresponds to maximum $C_L = 1.2761$, time = 99.30 units.
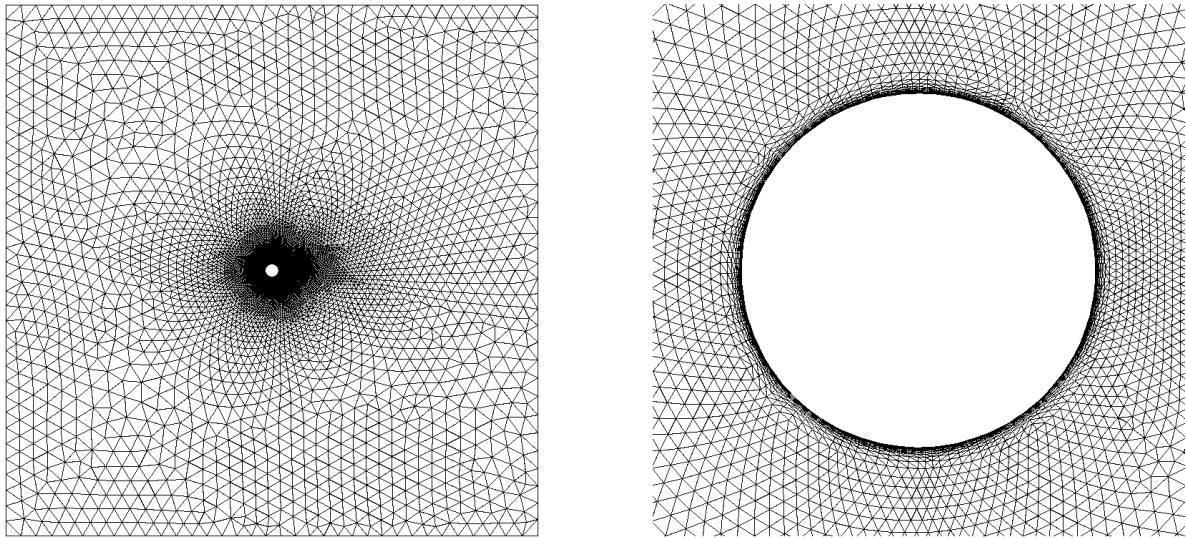
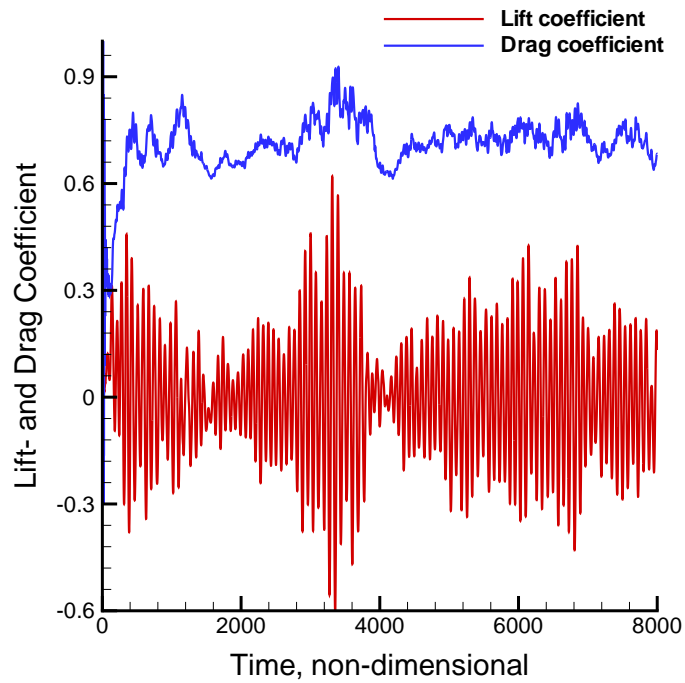**Figure 6. Side plane triangulation for the 4-to-1 cylinder grid containing 2,003,873 tetrahedral cells.**

Figure 7. History of the lift and drag coefficients for the DES-based computation of the unsteady flow over circular cylinder at M$_\infty$ = 0.1, α = 0°, Re$_D$ = 140,000.
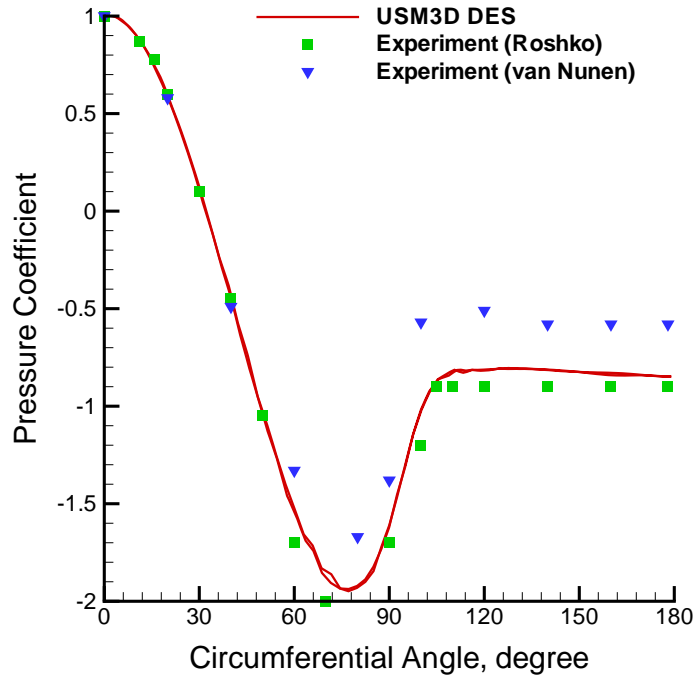
American Institute of Aeronautics and Astronautics Paper 2004-5201

Figure 8. Comparison of the time-averaged surface pressure coefficients corresponding to the DES-based computation and two experiments (digitized from Ref. [23]) for the circular cylinder at $M_\infty = 0.1$, $\alpha = 0^\circ$, $Re_D = 140,000$. Time averaged $C_D = 0.69$.
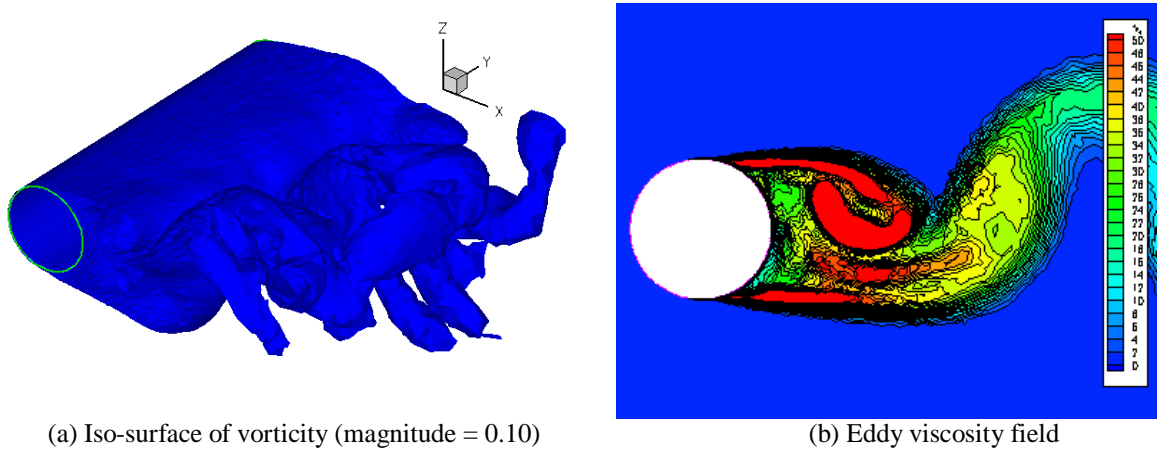

(a) Iso-surface of vorticity (magnitude = 0.10)

(b) Eddy viscosity field

Figure 9. Instantaneous views of the vorticity and eddy viscosity fields corresponding to the DES-based computation for the circular cylinder at $M_\infty = 0.1$, $\alpha = 0^\circ$, $Re_D = 140,000$.
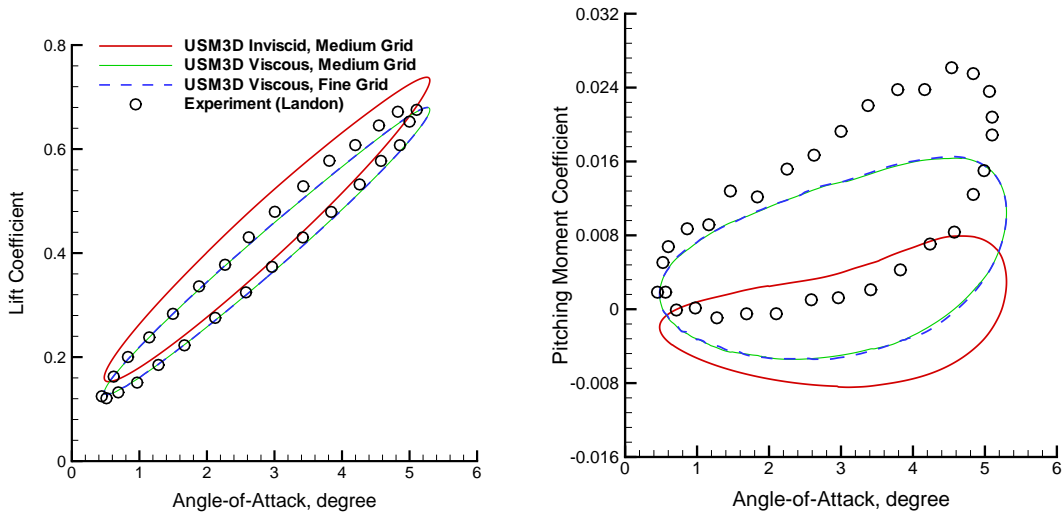
Figure 10. Comparison of computed and measured variation of lift and moment coefficients for NACA 0012 airfoil in a forced pitching oscillations at $M_\infty = 0.6$, $Re_c = 4.2 \times 10^6$. $\alpha(t) = \alpha_{mean} + \alpha_{ampl}\sin(2\pi f t)$, $\alpha_{mean} = 2.89°$, $\alpha_{ampl} = 2.41°$, $f = 50$ Hz.

(a) Minimum pitch angle ($\alpha = 0.48°$)   (b) Maximum pitch angle ($\alpha = 5.3°$)
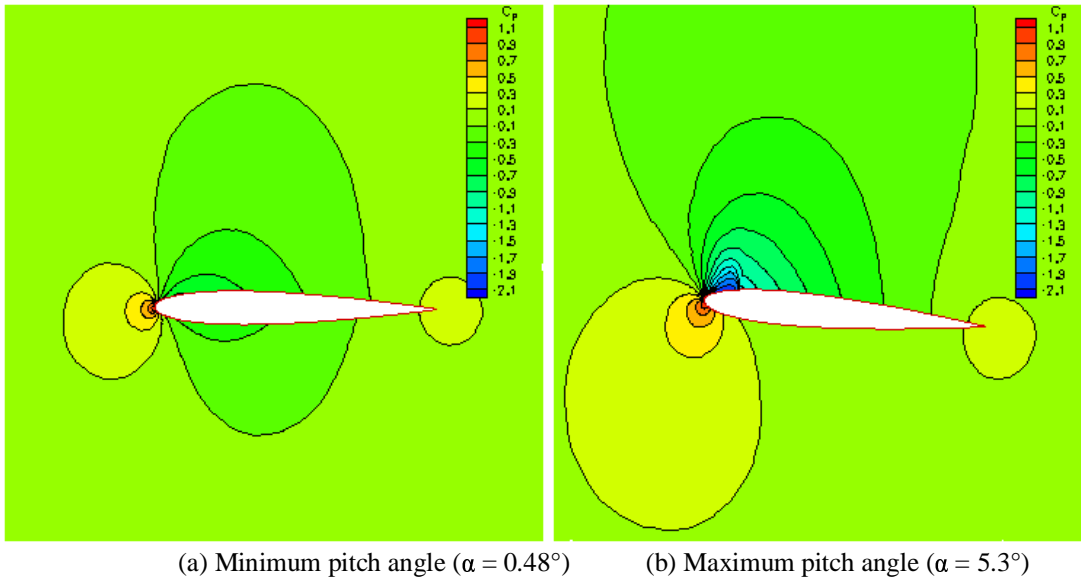
Figure 11. Contours of pressure coefficient in the near field of the NACA 0012 airfoil computed based on viscous simulation using the medium grid. $M_\infty = 0.6$, $Re_c = 4.2 \times 10^6$. $\alpha(t) = \alpha_{mean} + \alpha_{ampl}\sin(2\pi f t)$, $\alpha_{mean} = 2.89°$, $\alpha_{ampl} = 2.41°$, $f = 50$ Hz.